Spring 2020

Convergent Synthesis of Anaephene B

Mason A. Baber
Rollins College, mbaber@rollins.edu

Convergent Synthesis of Anaephene B

Mason A. Baber

A Senior Honors Project Submitted in Partial Fulfillment of the Requirements of the Honors Degree Program and Honors in the Major Field

April 2020

Faculty Advisor: Dr. James D. Patrone

Rollins College
Department of Chemistry

Winter Park, FL

Abstract

As strains of bacteria continuously evolve and become resistant to modern antibiotics, there exists a need for the development of new treatments to combat bacterial infection. *Staphylococcus aureus* (*S. aureus*) is known to develop such resistance and remains a leading cause of invasive infections and biofilm formation on prosthetic medical devices. In 2018, Brumley and Spencer *et al*. isolated anaephenes A–C, natural products from a marine bacterium. Anaephene B was of particular interest as it was the only member of the series to demonstrate moderate antibacterial activity against *S. aureus* (MIC = 6.1 μg/mL). Because of the potential clinical utility of anaephene B, investigation into synthetic production was warranted. A convergent synthesis of anaephene B will allow for production of the natural product and facile diversification in the production of analogs containing varied substituents on the aromatic ring and alterations in length, composition, or saturation of the aliphatic side chain. All analogs will be assayed against *S. aureus* in an investigation into the effects of structural modifications on antibacterial activity.

Introduction

Staphylococcus Aureus

For hundreds of years, *Staphylococcus aureus* (*S. aureus*) has been an evolving and dangerous pathogen in humans.[1] The phenotype of the bacteria is a sphere with a gold pigmentation that tends to aggregate in clusters.[2] *S. aureus* is gram-positive, indicating the presence of a thick cell wall, and also tests positive for coagulase, an enzyme that causes coagulation of the blood or plasma by converting fibrinogen, a soluble protein, to fibrin, an insoluble protein that forms a mesh-like structure and impedes blood flow.[2] About 30% of the human population are colonized by *S. aureus* and several studies have found that 10–20% of the population are consistently colonized.[2–4]

Despite there being an abundance of resident bacteria composing the microbiota of the human skin, including some species of staphylococci, *S. aureus* is not native to the skin microbiota and its primary competitor of the region is *S. epidermidis*.[5] Several mechanisms are in place to combat the colonization of the skin by foreign species. For instance, the resident bacteria of the skin act to protect the body through nutrient competition, competitive binding to epithelial cells, and by producing antimicrobial peptides and enzymes.[5,6] Lysozymes, enzymes found in human fluids and secretions, exhibit hydrolytic activity that can break down specific foreign entities; antimicrobial fatty acids produce and maintain the acid mantle, the acidic environment which is a signature feature of the human skin.[5] However, *S. aureus* exhibits resistance to several of these mechanisms, making it a dangerous adversary to the residents of the skin's microbiota.

Pathogenesis

Although *S. aureus* can establish a presence in and on several parts of the body, its primary reservoir is found in the nares, or the nostrils.[2] Staphylococci readily adhere or bind to endothelial

cells, which line the organs and cavities of the body, through various adhesin-receptor interactions.[2] The function of many *S. aureus* surface proteins is not known, but a class of surface proteins known as microbial surface components recognizing adhesive matrix molecules (MSCRAMMs) mediate attachment to and interaction with host cells.[7] MSCRAMMs can bind to ligands through a dock, lock, latch (DLL) mechanism or a protein specific mechanism known as the collagen hug (**Figure 1**).[7]

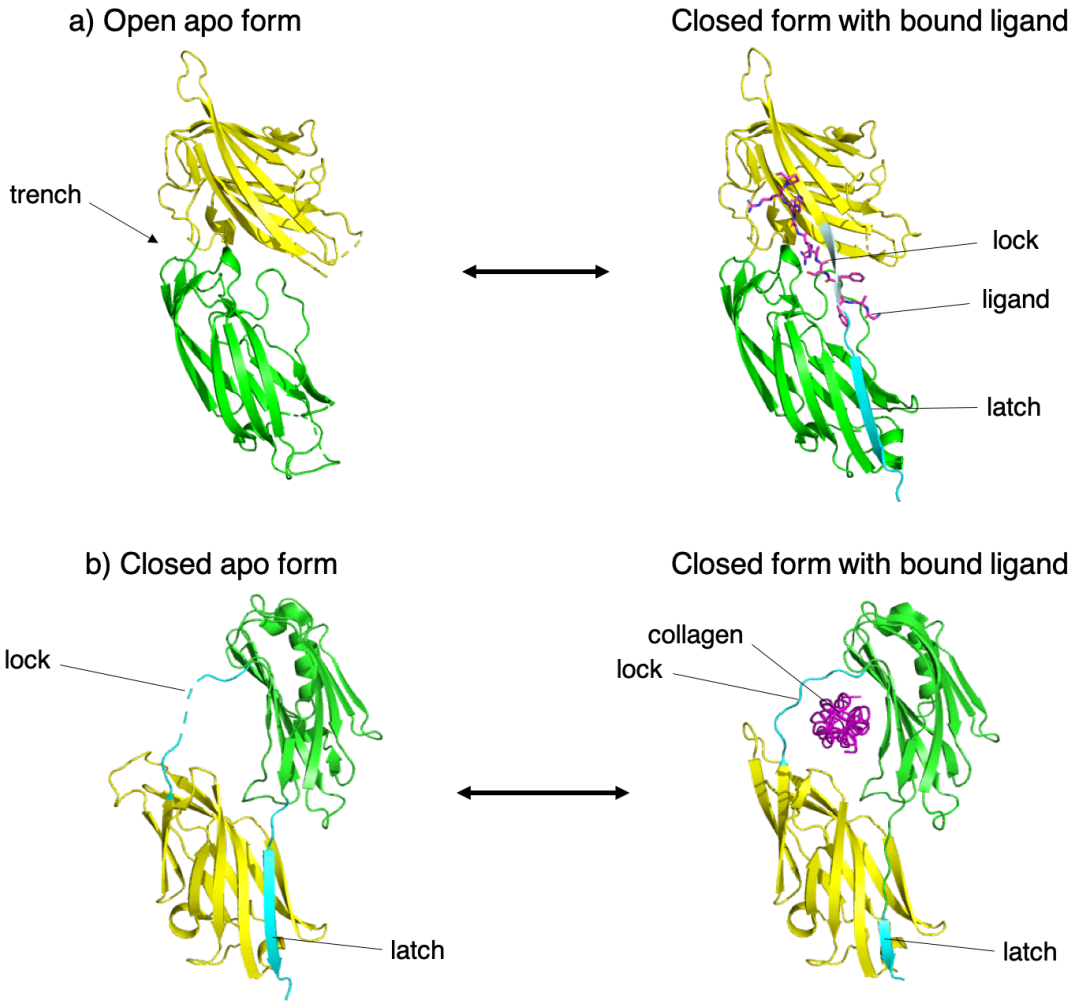

Figure 1. Mechanisms of ligand binding for MSCRAMM proteins.[7] a) Dock, lock, latch (DLL) mechanism. b) Collagen hug mechanism.

In the DLL mechanism, a ligand enters a trench within the MSCRAMM protein and induces a conformational change that causes the ligand to be locked in place by portions of the

protein acting as a latch.[7] The collagen hug mechanism is similar in that collagen enters the trench of the protein and a conformational change captures or "hugs" the collagen using residues of the locking domain of the protein.[7]

The pathogenesis of *S. aureus* begins with the attachment or adhesion of the bacteria either directly to an endothelial cell or to a site of damage where platelet-fibrin thrombi have formed (**Figure 2**). Phagocytosis allows the bacteria to enter the cell and release proteolytic enzymes which facilitate the spread of infection to nearby cells and tissue and reintroduction into the bloodstream. After phagocytosis, endothelial cells will begin to express surface receptors such as F_c receptors, intercellular, and vascular cell adhesion molecules to mediate the attachment of leukocytes upon release of interleukin-1, -6, and -8. Inflammatory response by endothelial cells will also result in abscess formation, leading to the development of infection and pathogenesis of diseases such as infective endocarditis and the formation of biofilms on prosthetic devices such as pacemakers or catheters.[3]

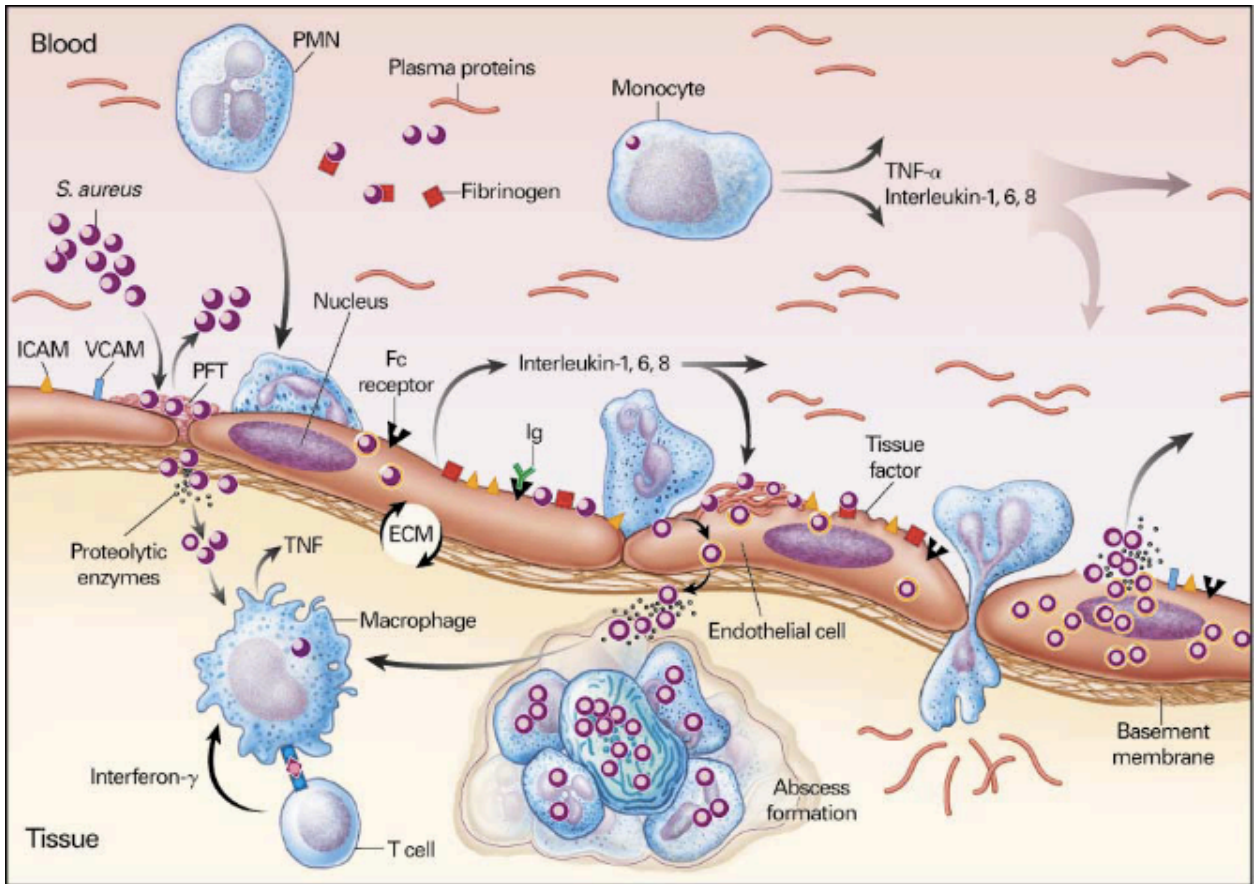

Figure 2. Invasion of tissue by *S. aureus*. ICAM: intercellular adhesion molecule; VCAM: vascular cell adhesion molecule; PFT: platelet-fibrin thrombi; ECM: extracellular matrix; TNF: tumor necrosis factor; PMN: polymorphonuclear leukocyte.[2]

Treatment

Antibiotics have long been the premier treatment option for combatting bacterial infections like *S. aureus*. The discovery and use of penicillin, the first β-lactam employed against *S. aureus*, greatly improved the prognosis of patients suffering from bacterial infections.[8] Other β-lactams have been developed and used against *S. aureus* such as methicillin. However, widespread use of antibiotics has resulted in an increase in resistance to β-lactam drugs and the emergence of drug-resistant bacterial strains such as methicillin-resistant *S. aureus* (MRSA), causing difficulty in treating bacterial infections and underscoring the need for the development of new drugs and treatments.

S. aureus has evolved in several ways to preserve and protect itself against antibacterial drugs. Production of the β-lactamase enzyme eliminates the antibiotic activity of β-lactam drugs by hydrolyzing the β-lactam ring while penicillin binding proteins, anchored in the cell wall, capture drug molecules (**Figure 3**).[2,8] Thickening of the cell wall can also contribute to drug resistance by reducing diffusion of drug molecule into the cell.[8] As more strains of *S. aureus* became resistant to common antibiotics, the use of the glycopeptide vancomycin rose and the bacteria remained relatively sensitive to the drug.[4,9] However, *S. aureus* is suspected to have received a transfer of high-level vancomycin resistance from *Enterococcus*, endangering the reliable use of vancomycin as an antibiotic against drug-resistant strains of the bacteria.[4,9]

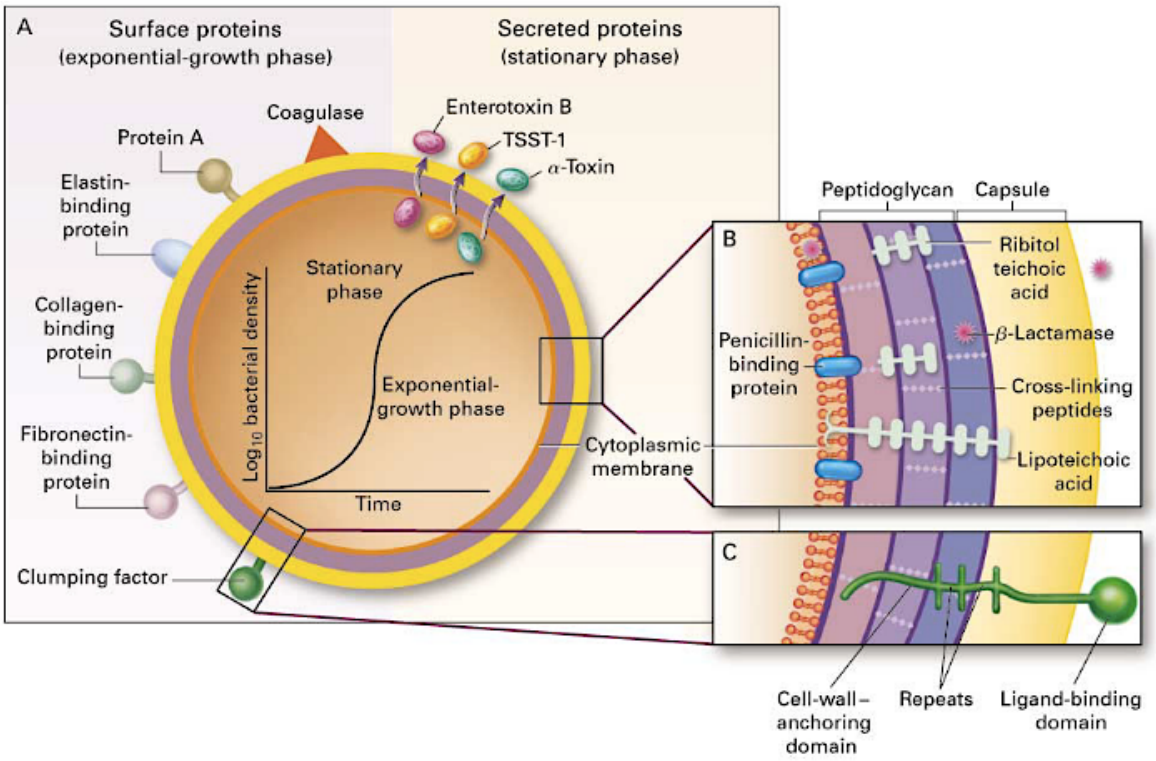

Figure 3. Structure of a *S. aureus* bacterium. Panel A shows a global view of the bacterium with labeled surface proteins and secreted proteins. Panel B shows a cross section of the cell envelope, comprised of peptidoglycan, which houses various cell structures, and an outer capsule layer. Panel C shows a general schematic of the anatomy of a cell-wall anchored protein. TSST-1: toxic shock syndrome toxin 1.[2]

Because of the increasing prevalence of antibiotic resistance in bacteria, new antibiotics are being sought and alternative forms of treatment and prevention, such as and anti-adhesives and vaccines, are being investigated.[10,11] Adhesion is a fundamental step toward colonization and, therefore, if adhesion can be inhibited or prevented, colonization can be reduced or prohibited. Furthermore, an approach focused on prevention of colonization rather than elimination provides an advantage in that the evolutionary pressure on the bacteria is reduced.[12] Traditional approaches targeted at reducing microbial viability encourage rapid mutation to mitigate the effects of antibacterial drugs and to develop resistances, whereas inhibition of colonization leaves the bacteria vulnerable to an innate immune response. There are several mechanisms of action that can be used to classify anti-adhesive molecules: bacterial adhesion mimetics (class I), host cell receptor mimetics (class II), inhibition of biosynthesis of adhesins (class III) or host receptors (class IV), and the use of antibodies to target bacterial adhesins (class V).[10] Class I anti-adhesives mimic adhesin components of bacteria and competitively bind to host cells while class II inhibitors bind directly to the adhesin components and interfere with adhesin-host interactions.[13–15] The members of class III and IV inhibit the biosynthesis of adhesins and host surface receptors, respectively, which eliminates the opportunity for interaction between the bacteria and host.[16–18] Lastly, class V inhibitors are antibodies that interfere with host cell recognition by targeting adhesins.[12]

Development of antibacterial vaccines, on the other hand, aims to institute a more definitive prevention method than anti-adhesives by providing full and durable protection from staphylococcal diseases. Targeted antigens in vaccine development often involve microbial surface proteins responsible for adhesion to host cells or biosynthetic pathways involved in the construction of the cell wall.[11,19,20] However, despite numerous preclinical studies, many lead candidates for *S. aureus* vaccines either never entered phase I clinical trials or were abandoned

shortly thereafter.[11] Two phase III trials were interrupted due to ambiguity between patients who received treatment and a placebo and reports of mortality in subjects.[11] As of 2018, no phase II clinical trials for *S. aureus* vaccines were active.[11] If achieved, a universal *S. aureus* vaccine would certainly be a major advancement in preventative medicine, but it is difficult to imagine such a treatment due to the multitude of staphylococcal antigens and the complexity and variety of the pathogenesis of the bacteria. In response, individual vaccines for each type of staphylococcal infection have been proposed, eliciting unique immune responses dependent upon factors such as the anatomical site of infection.[19]

Cyanobacteria

Nature often produces complex and diverse chemical structures and profiles easily, whereas synthetic production of compounds can be rather difficult. In the search for novel medicinal agents, natural products from a variety of sources including plants, bacteria, and fungi have become a huge area of interest and inspiration. In recent decades, pharmaceutical research has been in the midst of a renaissance in which natural product isolation, synthesis, and optimization has reemerged as a prominent source of drug molecules.[21] Because microalgal species, such as cyanobacteria, are such an expansive, unexplored kingdom, they provide a rich source of discovery for drug candidates with a low rate of rediscovery (**Figure 4**).[22] The complex biosynthetic machinery of cyanobacteria produce some of nature's most interesting natural products while simultaneously allowing for their survival in some of Earth's most extreme climates.

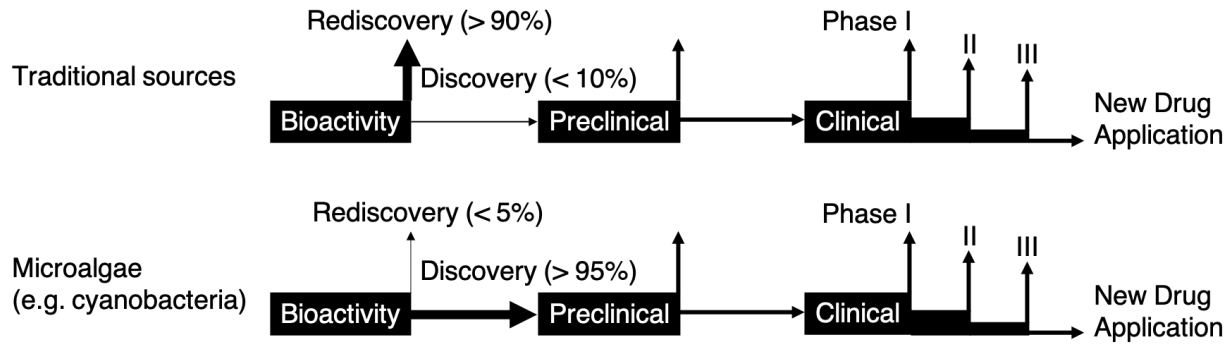

Figure 4. Comparison of drug development success from traditional and microalgal sources.[22]

Cyanobacteria are single-celled organisms capable of photosynthetic oxygen production and respiratory oxygen consumption and can survive in many extreme environments ranging from hot, humid springs to arid deserts to the frigid tundra.[23,24] Their survivability has been attributed in part to their production of diverse secondary metabolites which, in turn, has become a grand source of industrially relevant natural products.[24] Compounds produced by cyanobacteria have found promising application as biofuels, food supplements, and bioplastics.[25–27] Additionally, their production of bioactive molecules has created a potential for a wide array of pharmaceutical applications as the secondary metabolites of cyanobacteria have exhibited antibacterial, anticancer, and antiviral activity as well as inhibition of proteases and immunomodulatory activity.[21,28] Several natural products isolated from cyanobacteria have demonstrated antibacterial activity against *S. aureus* (**Figure 5**).[29–31] A series of chlorinated paracyclophanes **1–3**, known as carbamidocyclophanes

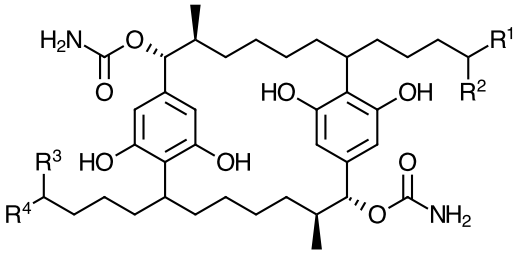

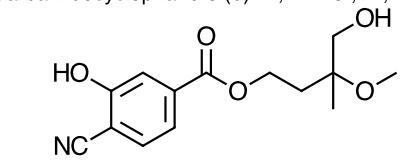

purified compound from *Nostoc muscorum* (**4**)

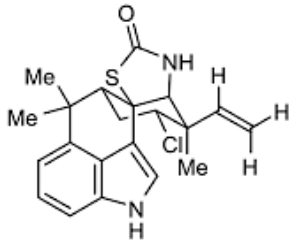

Hapalindole T (**5**)

Figure 5. Various natural products isolated from cyanobacteria.

A–C, isolated from a cyanobacteria found in northern Vietnam, *Nostoc* sp., strain CAVN 10, exhibited moderate antibacterial activity against *S. aureus*.[29] Similarly, a phenolic compound **4** isolated from *Nostoc muscorum* inhibited the growth of *S. aureus* and Hapalindole T (**5)**, isolated from *Fischerella* sp., demonstrated impressive inhibition of *S. aureus* with an MIC value of 0.25 µg/mL.[30,31] As a result of the multitude of reports of antibacterial activity from cyanobacteria metabolites, there has been a growing interest in discovering and optimizing their pharmaceutically relevant natural products.

Anaephene B

In 2018, Brumley and Spencer *et al*. reported on the isolation and characterization of a trio of natural products, known as anaephenes A–C (**6**–**8**), from a cyanobacterium of the marine genus *Hormoscilla*.[32] Extraction of 10.81 g of freeze-dried material yielded only minute amounts of **6**–**8** (8.3 mg, 0.5 mg, and 0.4 mg, respectively). Nevertheless, structural elucidation via spectroscopic methods revealed that the anaephenes were alkylphenols, each containing a different side chain with varying degrees of unsaturation. All three sport an alkene at C-5', but anaephene B contains a terminal alkyne and anaephene C has an additional alkene along the side chain (**Figure 6**).

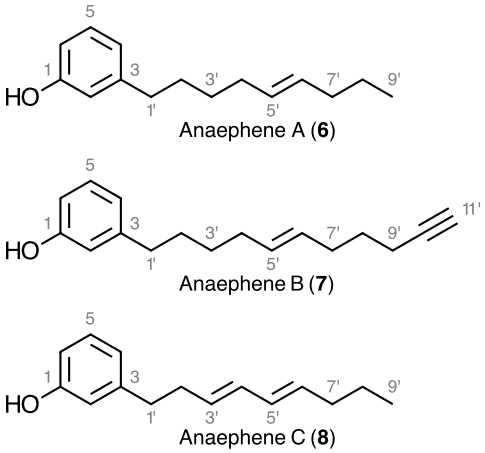

Figure 6. Structures of anaephenes A–C.

Production of compounds containing terminal alkynes and long, unsaturated alkyl chains is not uncommon for cyanobacteria and many of these natural products display biological activity. Pitipeptolide A, for example, contains a terminal alkyne and inhibits the growth of some strains of *Mycobacterium tuberculosis*.[33] Jamaicamide B also contains a terminal alkyne, but instead exhibits

sodium channel blocking activity.[34] Long alkyl chains with varying degrees of unsaturation have also been reported metabolites from cyanobacterium and have demonstrated potential as medicinal agents through inhibition of enzymatic activity, for instance.[35,36] The closest structural relatives to **6**–**8** are the hierridins, compounds isolated from the marine cyanobacterium *Phormidium ectocarpi*, which contain phenols from which long aliphatic tails extend.[37,38]

Because natural products often display potential for medicinal applications, the anaephene series was assayed for antimicrobial activity against several prominent bacterial targets. The most notable activity was demonstrated by **7**, with a 6.1 μg/mL MIC value against *S. aureus*.[32] Compounds **6** and **8** showed weak or insignificant activity against the assayed bacteria and all three compounds exhibited insignificant activity against selected cancer cell lines.[32] As a result, **7** emerged as a potential candidate for synthesis and optimization to improve its antibacterial activity and potential for medicinal application.

Initial Retrosynthetic Analysis

In the initial retrosynthetic analysis, the structure of **7** was divided into three fragments, which created the need to form two C–C bonds, both between sp^2 and sp^3 hybridized carbons (**Figure 7**). To accomplish C–C bond formation between the fragments, the synthesis was centered around Suzuki couplings. The base materials consisted of two alkyne compounds, one which will provide the terminal alkyne and one that can be transformed to contain a vinyl pinacol boronic ester which could serve as a coupling partner. Because both the alkyl halide and boronic ester will be primary (i.e. attached to only one carbon), a Suzuki coupling should result in a thermodynamically favored *trans* double bond. The phenol fragment, containing another pinacol boronic ester in the *meta* position, could be coupled to the constructed chain after it is activated by the installation of some halide.

Although the primary goal of the synthesis was to produce **7**, the potential for creation of analogs must also be considered. Due to the convergent methodology, diversification will likely involve alteration in starting materials. For instance, the substituent(s) of the aromatic ring could be changed or moved, and the length of the aliphatic starting materials could be adjusted.

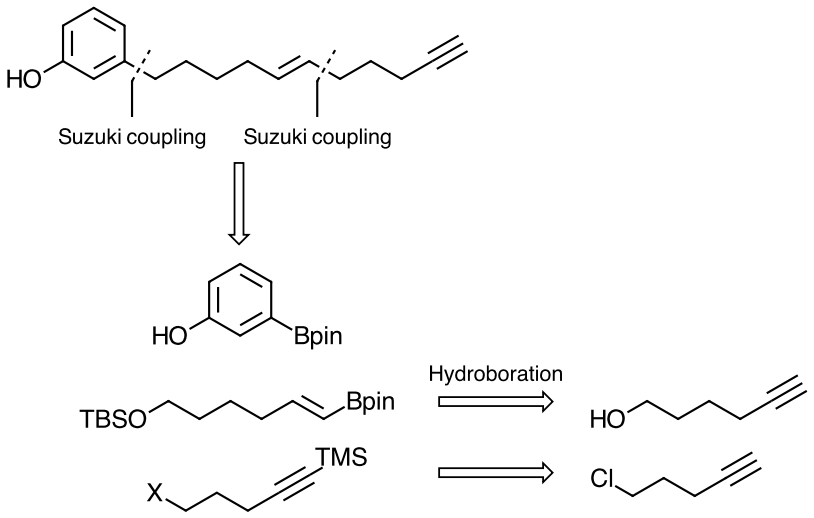

Figure 7. Initial retrosynthetic analysis of anaephene B. The target product is shown at the top, with dashed lines breaking the compound into three fragments which are shown below. The aromatic pinacol boronic ester was commercially available whereas the starting materials for the other two proposed fragments are shown at the end of the scheme.

C–C Bond Formation

Suzuki Coupling

The long aliphatic chain extending from the aromatic ring complicated the synthesis because of the absence of any functional groups that could be used as points of attachment via methods such as nucleophilic attack, coupling, or reduction. It is also well known that C–C bonds are difficult to make, and the saturated hybridization of the aliphatic chain only made this more challenging. To address this obstacle while also implementing the potential for diversification of the molecule, an initial convergent synthesis was proposed that involved a series of Suzuki couplings, one of the most common and powerful methods for C–C bond formation.

Cross-couplings are among the most popular options for constructing a C–C bond, which utilize a metal catalyst to facilitate bond formation. Coupling chemistry has an extensive history, dating back to the 19th century when Charles Wurtz reported on the homodimerization alkyl halides in the presence of sodium.[39] However, one of the most widely used modern coupling reactions did not emerge until the 1970s when Akira Suzuki reported on the palladium-catalyzed cross-coupling between aryl halides and organoboranes.[40]

Suzuki coupling generally occurs between an organohalide and an organometallic coupling partner, usually an organoborane, in the presence of a palladium catalyst and a base (**Figure 8**).[41] The mechanistic pathway begins, like many cross-coupling reactions, with an oxidative addition step in which the palladium catalyst is oxidized from Pd(0) to Pd(II) as it inserts between the halogen and its respective alkyl group. At this point, the base, generally an ionic species, participates in a metathesis step where the anionic component of the base replaces the halogen in the palladium complex and a salt is formed as a byproduct. The next step in the cycle requires the activation of the organoborane through a process similar to the aforementioned metathesis step in which the anionic component of the base bonds to the borane and forms a negatively charged species, the borate. Once the organoborane has been activated into a borate species, transmetallation can occur in which an alkyl species of the organoborane is transferred to the palladium complex and the boron forms a bond instead with the base component that was attached to the palladium. The final step, reductive elimination, involves the reduction of Pd(II) to Pd(0), the exit of the palladium from between the alkyl species, and the desired C–C bond formation. The completion of the cycle restores the starting catalyst which can participate in the cycle again.

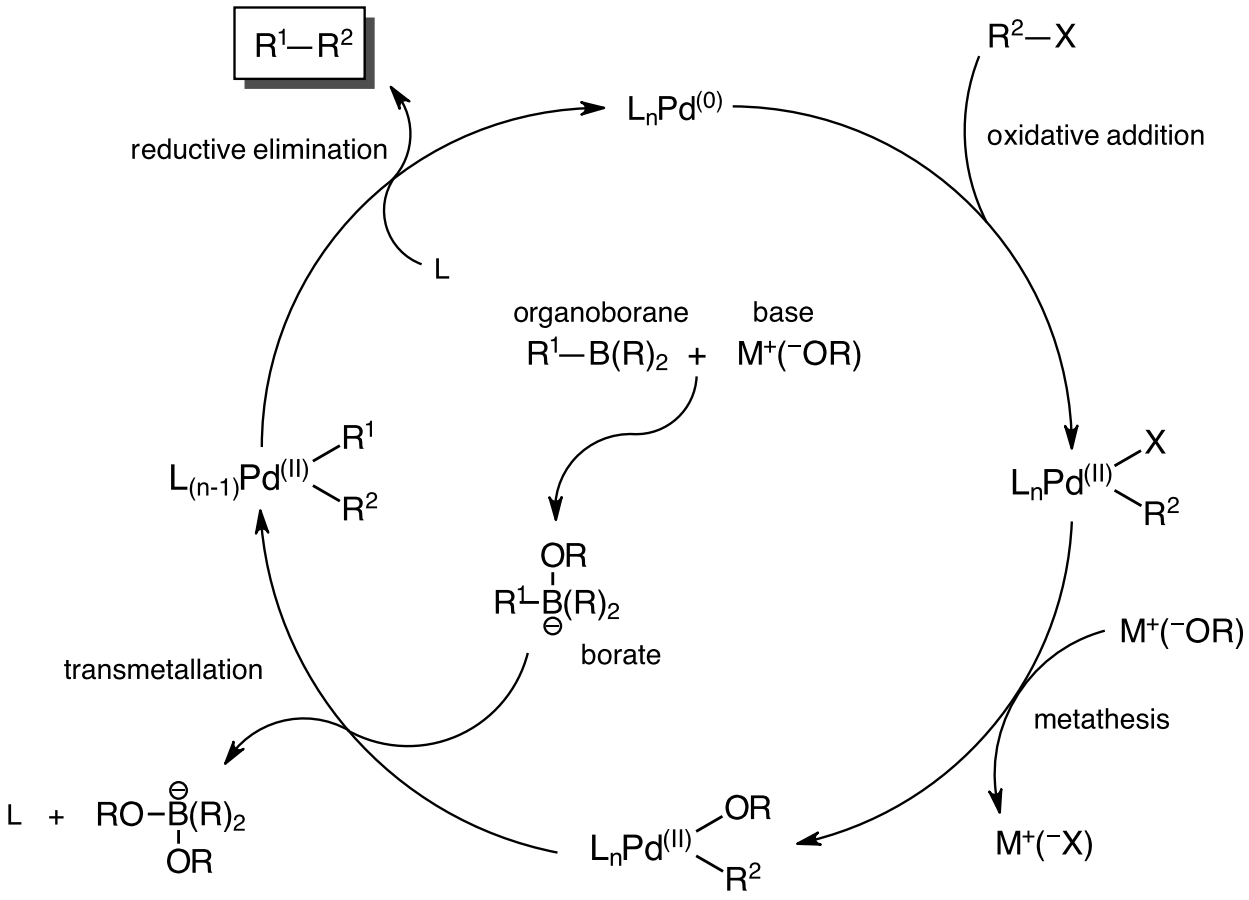

Figure 8. General mechanism of a Suzuki coupling.[41]

Preliminary Results

Synthetic Development

The initial synthetic pathway for the total synthesis of **7** involved Suzuki couplings for both the construction aliphatic chain and the attachment of the chain to the aromatic ring (**Scheme 1**). The alcohol of commercially available **9** was protected and the terminal alkyne was subjected to a Schwartz hydrozirconation to install a vinyl boronic ester. The Suzuki coupling was attempted with both commercially available **12** and synthesized TMS-protected 5-iodopent-1-yne **13b**. One attempt was also made with 5-iodopent-1-yne **13a**, which did not contain a protecting group on

the terminal alkyne. However, coupling of the boronic ester and alkyl halide always proved unsuccessful in yielding **14**.

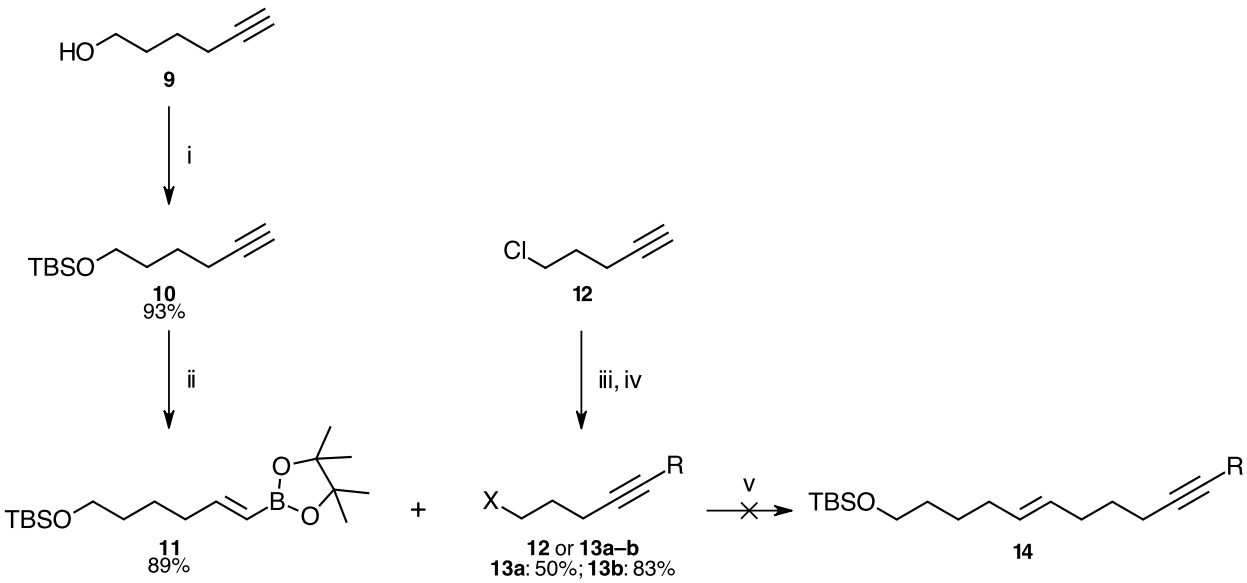

Scheme 1. Generation 1 of synthesis using Suzuki coupling to construct aliphatic chain. (i) TBSCl, imidazole, DCM; (ii) HB(pin), $HZrCp_2Cl$, 60 ºC, neat; (iii) for **Table 1**, entry 1–3: N/A; for **Table 1**, entry 5–14: nBuLi, THF, -78 ºC, TMSCl; (iv) for **Table 1**, entry 1–3: N/A; for **Table 1**, entry 5–14: NaI, acetone, reflux, 24 h; (v) variable, refer to **Table 1**.

The reaction was attempted with varied palladium sources, ligands, bases, and temperatures (**Table 1**). Despite this, the desired product was never successfully synthesized. A hypothesis for the failure of entries 1–4 (**Table 1**) is the occurrence of agostic interactions between the exposed terminal alkyne and the palladium catalyst, resulting in no reaction or an amalgam of undesired side products. With this in mind, entries 5–14 (**Table 1**) included a protected terminal alkyne and the halide was kept as an alkyl iodide in order to elevate the reactivity of the coupling partner, especially since it was an sp^3 hybridized halide which is uncommon in Suzuki reactions.

Table 1. Attempted coupling conditions for the joining of aliphatic chain fragments.

Entry	Compound	X	R	Catalyst	Ligand	Base	Temperature (ºC)
1	**12**	Cl	H	$Pd(dppf)Cl_2$	PCy_3	CsOH	60
2	**12**	Cl	H	$Pd_2(dba)_3$	PCy_3	CsOH	60
3	**12**	Cl	H	$Pd_2(dba)_3$	PCy_3	CsOH	90
4	**13a**	I	H	$Pd_2(dba)_3$	PCy_3	CsOH	90
5	**13b**	I	TMS	$Pd(dppf)Cl_2$	PCy_3	CsOH	60
6	**13b**	I	TMS	$Pd(dppf)Cl_2$	PCy_3	CsOH	90
7	**13b**	I	TMS	$Pd_2(dba)_3$	PCy_3	CsOH	60
8	**13b**	I	TMS	$Pd_2(dba)_3$	PCy_3	CsOH	90
9	**13b**	I	TMS	$Pd_2(dba)_3$	PCy_3	K_3PO_4	r.t.
10	**13b**	I	TMS	$Pd_2(dba)_3$	–	CsOH	90
11	**13b**	I	TMS	$Pd_2(dba)_3$	–	K_3PO_4	90
12	**13b**	I	TMS	$Pd_2(dba)_3$	–	Cs_2CO_3	90
13	**13b**	I	TMS	$Pd(PPh_3)_4$	–	K_3PO_4	r.t.
14	**13b**	I	TMS	$Pd(PPh_3)_4$	–	K_3PO_4	60

Table 1. Entries 1–3 were commercially available 5-chloropent-1-yne. The alkyl iodide listed as entry 4 was synthesized from 4-pentyn-1-ol. Entries 5–14 were synthesized from 5-chloropent-1-yne.

Each attempt resulted in either no reaction, as indicated by the apparent presence of starting material, or the generation of an undesired product. For instance, when the reaction was attempted in dioxane at 90 ºC with $Pd_2(dba)_3$ and cesium hydroxide (**Table 1**, entry 10) there was a promising NMR spectrum which suggested the aliphatic chain was synthesized, but the TMS-protecting group was removed *in situ*. However, without a mass spectrometer, it was difficult to verify the suspected product. Another possibility may be the occurrence of a nucleophilic attack by the cesium hydroxide base where the iodide is replaced by a hydroxy group and, subsequently, a C–C bond was formed between the alkene and terminal alkyne.

Because it is the rate determining step of the catalytic cycle, absence of oxidative addition during the attempted Suzuki couplings likely led to the plethora of unsuccessful reactions. Traditional Suzuki couplings generally utilize sp^2 hybridized organohalides, such as an aryl halide, where there is a degree of electron deficiency, granting the opportunity for oxidation of the palladium. In using sp^3 hybridized alkyl halides, a lack of electron deficiency may have prohibited the oxidation of the palladium catalyst.

After no success from this synthetic route, the heavy use of coupling chemistry was reconsidered. The alternative approach (**Scheme 2**) included the replacement of a palladium-catalyzed coupling with an organomagnesium reagent, or Grignard reagent, which would allow for the attachment of the aromatic ring to a small aliphatic fragment. A magnesium insertion to form a Grignard reagent was performed on commercially available **15**, after which the electrophile, commercially available 4-bromobut-1-ene, was added. However, the NMR spectra obtained from attempted reactions suggested that the Grignard was being quenched, but the cause of the quenching required additional pontification. It was hypothesized that the electrophile, 4-bromobut-1-ene, was slightly too acidic due to an inductive effect caused by the bromide. The quenching of the Grignard by this electrophile would result in a TBS-protected phenolic species and a hydrocarbon, potentially the very stable 1,4-butadiene.

To construct the other fragment, which was planned to serve as an sp^2 hybridized alkyl halide coupling partner in another Suzuki reaction, commercially available 1,6-heptadiyne **18** was subjected to a monoprotection with a TIPS group to afford **19**. The TMS group that had previously been employed for the protection of the terminal alkyne was exchanged for TIPS as it is a larger protecting group that would ensure durability and grant additional steric protection for the alkyne. However, the activation of the unprotected terminal alkyne using a Schwartz hydrozirconation to install a vinyl iodide **20** was unsuccessful. Upon reflection, the transformation of **19** to **20** potentially failed due to the use of a catalytic, rather than stoichiometric, amount of the Schwartz reagent. Although a catalytic Schwartz hydrozirconation was previously employed to install a vinyl pinacol boronic ester (**Scheme 1**), the HB(pin) provided a proton to restore the catalyst. In attempting to install a vinyl iodide, elemental iodine was used and, therefore, there was no additional proton available to restore the catalyst.

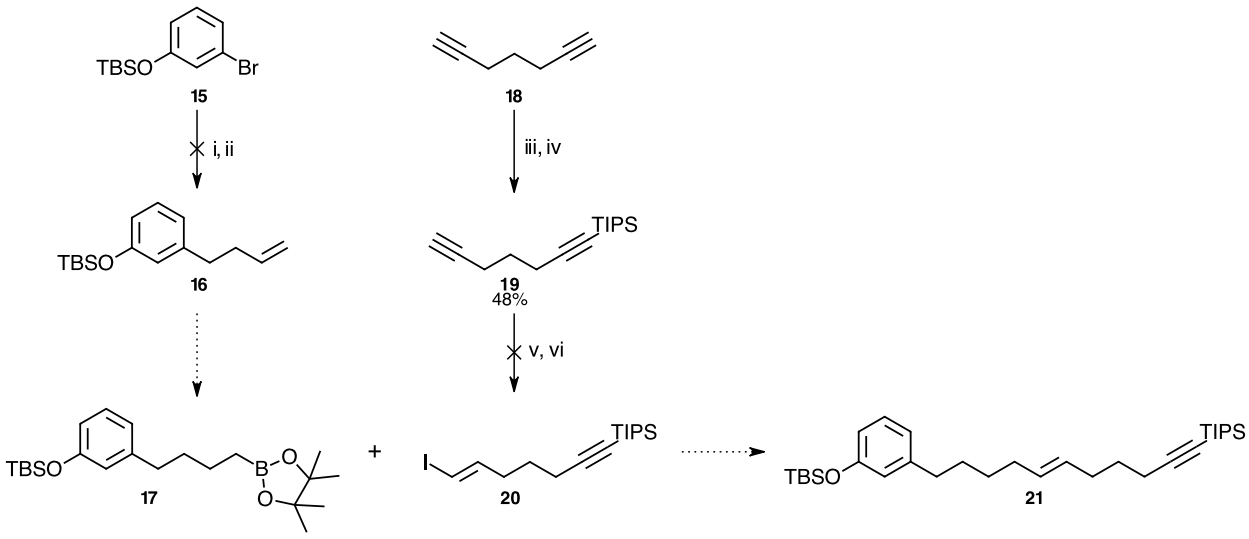

Scheme 2. Generation 2 of synthesis using a Grignard reagent to build from aromatic ring. (i) Mg, ether or THF, r.t–reflux; (ii) 4-Bromobut-1-ene, THF, 0–60 ºC; (iii) LiHMDS, THF, -78 ºC; (iv) TIPSCl, -78 ºC; (v) $HZrCp_2Cl$, THF, 60 ºC. (vi) I_2, THF, -25 ºC.

To address the acidity of the electrophile in the Grignard reaction, 4-bromobut-1-ene was exchanged for a less acidic alkyl species that would allow for coupling off the same fragment **22** without further modification or activation **(Scheme 3**). However, the reaction proved unsuccessful after insertion of the magnesium within the C–Br bond was not achieved as indicated by an NMR spectrum showing the aryl bromide starting material.

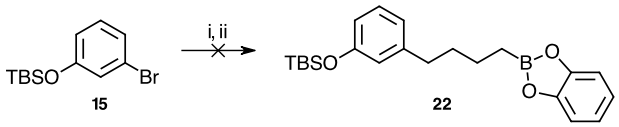

Scheme 3. Attempted alternate Grignard reaction with a less acidic electrophile. (i) Mg, THF, reflux; (ii) 2-(4-Bromobutyl)-1,3,2-benzodioxaborolane, THF.

Due to the difficulties in synthesis that arose from the sensitivity of the aryl Grignard reagent and the failure in constructing the rest of the aliphatic chain from **18**, a new retrosynthetic analysis was performed (**Figure 9**). The target compound **7** was divided into two fragments, which were planned to be joined via a Suzuki coupling. The left half of the molecule was prepared using a Grignard reaction, but with a proper difference in acidity between the electrophile and nucleophile. In preparing an organohalide coupling partner, the hybridization of the alkyl halide was important to consider. A Takai olefination of an aldehyde would yield a primary vinyl iodide,

granting a higher degree of electron deficiency for the organohalide compared to that seen in the initial retrosynthetic analysis.

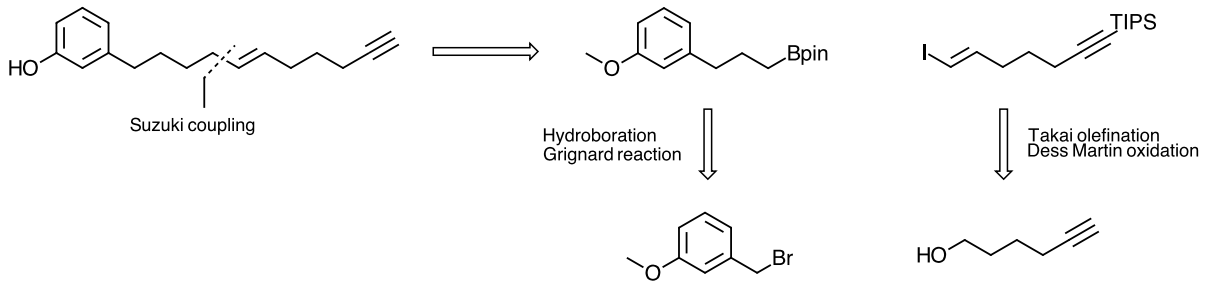

Figure 9. Revised retrosynthetic analysis of anaephene B. The target product, shown on the left, was divided into two fragments, seen on the right. Both starting materials were commercially available and could be used to prepare a vinyl iodide and pinacol boronic ester to be used in a Suzuki coupling.

Beginning with commercially available starting materials, a Grignard reaction and Takai olefination were used to accomplish the construction of fragments appropriate for a Suzuki coupling (**Scheme 4**). Because the magnesium insertion to form an aryl Grignard reagent was proving unreliable, the revised scheme utilized commercially available allylmagnesium bromide. Using **23** as the electrophile, a Grignard reaction produced alkene **24**, which was subjected to a hydroboration to yield pinacol boronic ester **25**. To synthesize the organohalide coupling partner, commercially available **9** was subjected to a selective protection of the terminal alkyne before a selective oxidation of the alcohol to yield **26**. A Takai olefination produced vinyl iodide **20**, which can be used as the coupling partner for **25** in a Suzuki coupling to afford **27**. Removal of the TIPS protecting group will reveal the terminal alkyne and demethylation of the aryl methoxy will afford the desired phenol **7**.

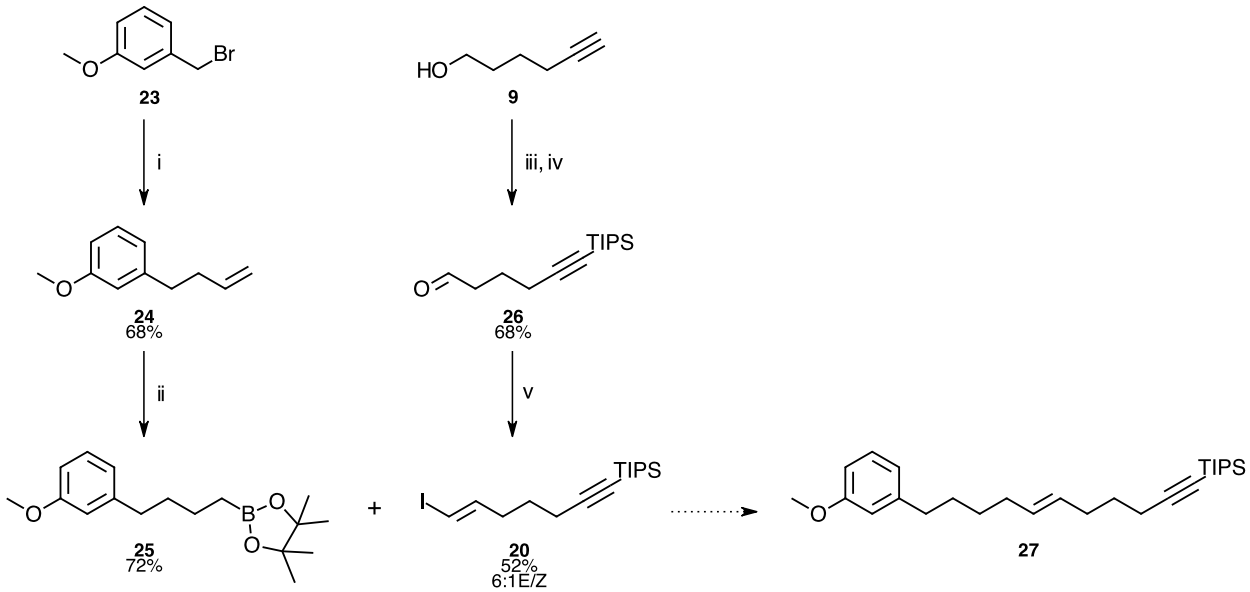

Scheme 4. Generation 3 of synthesis using a Grignard reaction and a Takai olefination in construction of aliphatic chain. (i) allylmagnesium bromide, THF; (ii) HB(pin), $H_3B{\cdot}THF$, 60 °C; (iii) ethylmagnesium bromide, TIPSCl, THF, reflux; (iv) DMP, DCM (v) $CrCl_2$, CHI_3, dioxane/THF.

With the revisions to the Grignard reaction, the synthesis of the pinacol boronic ester **25** was accomplished easily. However, the newly incorporated Takai olefination proved much more difficult and required extensive investigation to achieve a productive reaction followed by optimization of conditions to favor production and isolation of the *E* isomer of the alkene product **20** (**Table 2**). Equivalents, solvent, and addition protocols were the primary variables for creating productive, stereoselective reactions whereas workup protocols were modified to optimize isolation. Due to the similarity of the *E* and *Z* isomers, they were not able to be easily separated and, instead, stereoselective production of the *E* isomer was the favored approach for obtaining diastereomeric purity.

Table 2. Matrix of reaction conditions for the attempted Takai olefination of 26.

Entry	Equivalents **26**:CHI_3:$CrCl_2$	Solvent	Comments	Outcome
1	1:1.15:3	THF[a]	0 °C; concerted addition	SM
2	1:2:6	THF[a]	0 °C; concerted addition	Product (4:1 E/Z)
3	1:4:8	THF[a]	r.t.; stepwise addition	SM
4	1:2:8	6:1 dioxane/THF[a]	0 °C; stepwise addition	SM
5	1:2:8	6:1 dioxane/THF	0 °C; stepwise addition	Product (8:1 E/Z)
6	1:2:8	THF[a]	0 °C; stepwise addition	Product (6:1 E/Z)
7	1:2:8	THF[a]	0 °C; stepwise addition	Abandoned
8	1:2:8	1:1 dioxane/THF	0 °C; stepwise addition	Abandoned
9	1:1.15:6	6:1 dioxane/THF	0 °C; stepwise addition	Abandoned
10	1:1.15:6	6:1 dioxane/THF	0 °C; stepwise addition	Abandoned
11	1:1.15:8	THF	r.t.; stepwise addition	SM/product (6:1 E/Z)
12	1:1.15:8	THF	r.t.; stepwise addition; exposed to O_2	SM/product (6:1 E/Z)
13	1:3:10	6:1 dioxane/THF	r.t.; concerted addition; Cr/THF slurry[b]	Product (13:1 E/Z)
14	1:2:8	6:1 dioxane/THF	r.t.; concerted addition	Abandoned
15	1:2:8	12:1 dioxane/THF	r.t.; concerted addition	Abandoned
16	1:2:8	12:1 dioxane/THF	r.t.; concerted addition; Cr/THF slurry[b]	Product (10:1 E/Z)

Table 2. [a] Solvent used was not anhydrous. [b] One part THF was added to $CrCl_2$ to form a slurry and allow complexation before being solvated by dioxane. E/Z ratios refer to the stereoisomers of the alkene product as determined by ^1H NMR. SM: starting material. r.t.: room temperature.

Previously published methods commonly used THF to solvate the highly air and moisture sensitive chromium(II) chloride before adding a mixture of aldehyde and iodoform in THF either at 0 °C or ambient temperatures.[42–44] Other protocols used a dioxane/THF mixture by first solvating the chromium(II) chloride with THF, then adding dioxane, which tended to produce a more stereoselective reaction.[45,46]

When attempted with conservative equivalents in THF (**Table 2**, entry 1), the aldehyde did not successfully react, suggesting that a larger excess of iodoform and/or chromium was required. As equivalents were altered, it became clear the reaction was most likely to be successful when there were at least 2 equivalents of iodoform with respect to the aldehyde. Anhydrous solvent and inert atmosphere also appeared to influence the success, but may not be required as some trials

proved successful, nonetheless. For all attempts, the color of the reaction mixture was used as a qualitative marker to assess if the reaction was proceeding. Successful reactions tended to change from a grayish tone to a reddish brown, presumably due to creation of free iodide as a result of the methylene of iodoform complexing to the chromium species. Entries 3–12 (**Table 2**) investigated the effect of a stepwise addition (i.e. adding iodoform separate from aldehyde) on the success, but many of the trials were abandoned due to a lack of appropriate color change. The highest stereoselectivities of 13:1 of the desired Z isomer were achieved when a slurry of chromium(II) chloride in THF was created before adding a six- or twelve-fold amount of dioxane (**Table 2**, entries 13 and 16).

In addition to being difficult to separate from its *Z* stereoisomer, it was also troublesome to separate product **20** from other species in the reaction mixture including any residual chromium entities, iodoform, and free iodide produced as a result of both the successful reaction and the decomposition of the light-sensitive iodoform. The presence of chromium was noted by a green tint to the isolated oil but could generally be removed easily through column chromatography or filtration through silica or celite. Free iodide caused the isolate to exhibit a pink or purple color, which was also used as an indicator of the presence of iodoform. To remove free iodide, the workup protocols were adjusted to include copious amounts of sodium thiosulfate, but removal of iodoform required further experimentation. Due to the structure and properties of **20**, it was hypothesized that it should be highly soluble in the nonpolar solvent hexanes whereas the polar iodoform should be less soluble. Upon dissolving a crude isolate of **20** in hexanes, iodoform was observed to fall out of solution, especially at low temperatures, providing a facile method of removing the majority of iodoform from the product.

Future Directions

This project will progress through continued synthetic efforts to produce **7**, specifically by investigating the joining of fragments **20** and **25** via a Suzuki coupling and subsequent deprotection steps. The synthetic route proposed in **Scheme 4** allows for the facile production of the first analog of **7** by preserving the aryl methoxy rather than removing the methyl group to reveal the phenol. The synthesis of additional analogs will involve installing other moieties on the aromatic ring, such as an amino or nitro group, moving the phenol or methoxy around the ring, and altering the length and saturation of the aliphatic chain. All compounds will not only require full characterization, but also analysis of antibacterial activity against *S. aureus* to verify the reported activity of **7** and to investigate the effects of structural changes on those properties.

Experimental

General procedures. All reactions were performed in oven or flame-dried glassware using standard Schlenk techniques under a positive pressure of N_2 unless otherwise noted.

***tert*-Butyl-hex-5-ynoxy-dimethylsilane (10).** In air, compound **10** was prepared according to a previously published method with minor modifications.[47] Imidazole (1.04 g, 15.27 mmol) was dissolved in DCM (10 mL). To the stirring solution was added 5-hexyn-1-ol (0.56 mL, 5.09 mmol). After stirring for several minutes, TBSCl (1.15 g, 7.64 mmol) was added and the white cloudy solution stirred at r.t. overnight. The mixture was diluted with water and then extracted with DCM. The organic layer was dried over sodium sulfate and purified via column chromatography (3% ethyl acetate in hexanes) to yield the product as a clear, colorless oil (1.00 g, 93%). ^{1}H NMR (301 MHz, $CDCl_3$) δ 3.63 (t, J = 6.0 Hz, 2H), 2.25 – 2.18 (m, 2H), 1.94 (t, J = 2.7 Hz, 1H), 1.63 – 1.57 (m, 4H), 0.89 (s, 9H), 0.04 (s, 6H).

(E)-*tert*-Butyldimethyl((6-(4,4,5,5-tetramethyl-1,3,2-dioxaborolan-2-yl)hex-5-en-1-yl)oxy)silane (11). Hydroboration of **10** was accomplished according to a previously published method with minor modifications.[47] Compound **10** (500 mg, 2.35 mmol) was combined with 4,4,5,5-tetramethyl-1,3,2-dioxaborolane (HB(pin)) (274 mg, 2.14 mmol) and Schwartz's reagent ($HZrCp_2Cl$) (55 mg, 0.214 mmol) under an N_2 atmosphere. The reaction was heated to 60 ºC and allowed to stir overnight. The cloudy yellow solution was cooled to r.t. before being purified via column chromatography (3% ethyl acetate in hexanes) to produce the desired product as a clear, colorless oil (650 mg, 89%). ^{1}H NMR (301 MHz, $CDCl_3$) δ 6.70 – 6.56 (m, 1H), 5.42 (d, J = 18.0 Hz, 1H), 3.59 (t, J = 6.1 Hz, 2H), 2.16 (q, J = 7.2, 6.5 Hz, 2H), 1.54 – 1.44 (m, 4H), 1.26 (s, 12H), 0.88 (s, 9H), 0.03 (s, 6H).

5-Iodo-1-pentyne (13a). Iodination of 4-pentynol was performed according to a previously published method with minor modifications.[48] In air, solid iodine (1.96 g, 7.73 mmol) was ground into a powder and dissolved in DCM (25 mL). Triphenylphosphine (2.03 g, 7.73 mmol) and imidazole (526 mg, 7.73 mmol) were added to the mixture. To the stirring mixture, 4-pentynol (0.55 mL, 5.94 mmol) was added and the reaction stirred at r.t. for 2 h. The reaction was quenched with saturated sodium thiosulfate solution and the organic layer was washed twice with brine and dried over sodium sulfate before being purified via column chromatography (1% ethyl acetate in hexanes) to yield the desired product as a clear, colorless oil (570 mg, 50%). ^{1}H NMR (301 MHz, $CDCl_3$) δ 3.31 (t, J = 6.7 Hz, 2H), 2.34 (td, J = 6.8, 2.7 Hz, 2H), 2.05 – 2.00 (m, 1H), 2.01 – 1.97 (m, 2H).

5-Iodopent-1-ynyl(trimethyl)silane (13b). Compound **13b** was prepared according to previously published methods.[49] A solution of 5-chloropent-1-yne (308 mg, 3 mmol) in THF (3 mL) was cooled to -78 ºC using a liquid N_2/ethyl acetate bath. A solution of n-butyllithium (1.6 M in hexanes, 1.6 mL, 2.6 mmol) was added dropwise. After stirring for 10 min., a solution of trimethylsilyl chloride (1 M in DCM, 3 mL, 3 mmol) was added dropwise. The reaction mixture was allowed to slowly warm to r.t. and stir overnight. The cloudy white mixture was added to water and the aqueous layer was extracted three times with ethyl acetate. The organic layers were combined and washed once with brine, dried over sodium sulfate, and concentrated *in vacuo* to afford a yellow oil. Sodium iodide (1.12 g, 7.5 mmol) was dissolved in acetone (6.25 mL) and the solution was added to the crude silane. The clear yellow reaction mixture stirred at reflux (60 ºC) for 24 h and was then diluted with hexanes and washed with water twice. The organic layers were combined, dried over sodium sulfate, and concentrated *in vacuo* to yield the desired product as an orange oil (660 mg, 83%). ^{1}H NMR data were in agreement with those reported in literature.[49] ^{1}H NMR (301 MHz, $CDCl_3$) δ 3.29 (t, J = 6.8 Hz, 2H), 2.36 (t, J = 6.8 Hz, 2H), 2.00 (p, J = 6.8 Hz, 2H), 0.14 (s, 9H).

1,6-Heptadiyn-1-yltriisopropylsilane (19). Compound **19** was prepared according to previously published methods with minor modifications.[50] A solution of 1,6-heptadiyne (92 mg, 1 mmol) in THF (5 mL) was cooled to -78 ºC in a liquid N_2/ethyl acetate bath. A solution of lithium bis(trimethylsilyl)amide (1 M in THF, 1 mL, 1 mmol) was added dropwise and produced a yellow solution that stirred for 45 min. at -78 ºC. Triisopropylsilyl chloride (231 mg, 1.2 mmol) was dissolved in THF (0.5 mL) and added to the reaction mixture. The mixture stirred at -78 ºC for an additional 2 h before being quenched with saturated ammonium chloride solution (10 mL) and allowed to warm to r.t. overnight while stirring. The aqueous layer was extracted twice with ether and the organic layers were combined, dried over sodium sulfate, and purified via column chromatography (hexanes) to afford the desired product as a clear, colorless oil (120 mg, 48%). ^{1}H NMR (301 MHz, $CDCl_3$) δ 2.44 – 2.30 (m, 6H), 1.96 (t, J = 2.7 Hz, 1H), 1.75 (p, J = 6.7 Hz, 3H), 1.05 (s, 18H).

[(6*E*)-7-Iodo-6-hexen-1-yn-1-yl]tris(1-methylethyl)silane (20). A 20 mL reaction vial was charged with $CrCl_2$ (389 mg, 3.17 mmol) inside the glovebox. The $CrCl_2$ was flame dried under vacuum and allowed to cool to r.t. before THF (4 mL) was added and mixed for 10 min. A solution of aldehyde **26** (100 mg, 0.396 mmol) and iodoform (312 mg, 0.792 mmol) in dioxane (1 mL) was added. The reaction was protected from light with foil and stirred at r.t. overnight. The next day, the reaction was diluted with ether and washed with saturated sodium thiosulfate (5 x 30 mL),

water, and brine. The organic layer was collected, evaporated *in vacuo*, and purified via column chromatography (hexanes) to yield a clear oil (77 mg, 52%, *E*/*Z* 6:1). The *Z* isomer presents a doublet at δ 6.22 in the NMR spectrum. The *E*/*Z* ratio was calculated based on an integral ratio of the alkenyl protons. ^{1}H NMR (301 MHz, $CDCl_3$) δ 6.50 (dt, J = 14.5, 7.3 Hz, 1H), 6.03 (dt, J = 14.3, 1.4 Hz, 1H), 2.34 – 2.16 (m, 4H), 1.64 (dt, J = 14.5, 7.4 Hz, 2H), 1.05 (s, 21H).

4-(*m*-Methoxyphenyl)-1-butene (24). Compound **24** was prepared according to previously published methods.[51] To a solution of 3-methoxybenzyl bromide (140 µL, 1 mmol) and THF (1 mL) was added allylmagnesium bromide (1 M in diethyl ether, 2 mmol, 2 mL) dropwise. The opaque solution was allowed to stir overnight at r.t.. The reaction was quenched with saturated ammonium chloride solution (10 mL) and then diluted with DCM. The aqueous layer was extracted with DCM twice and the organic layers were washed with water once, dried over sodium sulfate, filtered through celite, and purified via column chromatography (hexanes) to yield the desired product as a clear, colorless oil (110 mg, 68%). ^{1}H and ^{13}C NMR data were in agreement with those reported in literature.[51] ^{1}H NMR (301 MHz, $CDCl_3$) δ 7.19 (t, 1H), 6.79 (d, J = 7.8 Hz, 1H), 6.75 – 6.71 (m, ovlp, 2H), 5.94 – 5.78 (m, 1H), 5.05 (dq, J = 17.1, 1.6 Hz, 1H), 5.01 – 4.95 (m, 1H), 3.80 (s, 3H), 2.69 (t, 2H), 2.37 (q, 2H). ^{13}C NMR (76 MHz, $CDCl_3$) δ 159.67, 143.63, 138.17, 129.34, 120.95, 115.04, 114.30, 111.14, 55.24, 35.51, 31.70.

2-[4-(*m*-Methoxyphenyl)butyl]-4,4,5,5-tetramethyl-1,3,2-dioxaborolane (25). Compound **25** was prepared according to previously published methods with minor modifications.[52] Compound **24** (162 mg, 1 mmol) was combined with HB(pin) (0.16 mL, 1.1 mmol) and H_3B·THF (1 M in THF, 0.1 mL, 0.1 mmol). The colorless mixture was heated to 60 °C and allowed to stir overnight. The reaction was diluted with hexanes and purified via column chromatography (2% ethyl acetate in hexanes) to yield a clear, colorless oil (210 mg, 72%). ^{1}H NMR (301 MHz, $CDCl_3$) δ 7.18 (t, J = 7.4 Hz, 1H), 6.79 – 6.68 (m, 3H), 3.79 (s, 3H), 2.58 (t, 2H), 1.66 – 1.57 (m, 2H), 1.53 – 1.42 (m, 2H), 1.24 (s, 12H), 0.84 – 0.77 (m, 2H). ^{13}C NMR (76 MHz, $CDCl_3$) δ 159.62, 144.69, 129.21, 120.94, 114.20, 110.90, 83.00, 55.14, 35.92, 34.17, 24.90, 23.87, 14.23.

6-Triisopropylsilanyl-hex-5-ynal (26). Compound **26** was prepared according to previously published methods with minor modifications.[53] To a solution of 5-hexyn-1-ol (1.12 mL, 10.2 mmol) in THF (20 mL) was added ethylmagnesium bromide (3 M in ether, 7 mL, 21.4 mmol) dropwise using a slow addition funnel. The light yellow reaction mixture was refluxed (60 °C) and stirred overnight. A solution of TIPSCl (2.18 mL, 10.2 mmol) in THF (2 mL) was added dropwise at r.t. and the cloudy solution was refluxed (60 °C) and stirred for 6 h. The clear reaction mixture was quenched with 3 M HCl and extracted with ethyl acetate. The organic layer was washed with brine, dried over sodium sulfate, and concentrated *in vacuo* to yield the protected alkyne as an oil. After being diluted with DCM (1 mL), the protected alkyne was added to a solution of Dess-Martin periodinane (4.54 g, 10.71 mmol) in DCM (35 mL). Water (0.192 mL, 10.71 mmol) was added and the cloudy white reaction mixture stirred at r.t. for 30 min before being poured into a 1:1 solution of sodium bicarbonate and sodium thiosulfate. The mixture was extracted with DCM and the organic layer was washed with saturated sodium bicarbonate once then with brine before being dried over sodium sulfate and purified via column chromatography (hexanes, then 10% ethyl acetate in hexanes) to afford a yellow oil (1.76 g, 68%). ^{1}H NMR (301 MHz, $CDCl_3$) δ 9.81 (t, J = 1.4 Hz, 1H), 2.62 (t, J = 7.3 Hz, 2H), 2.33 (t, J = 6.8 Hz, 2H), 1.85 (p, J = 7.0 Hz, 2H), 1.05 (s, 21H). ^{13}C NMR (76 MHz, $CDCl_3$) δ 202.04, 107.52, 81.63, 42.80, 18.71, 17.79, 12.36, 11.32.

Acknowledgements

Firstly, I would like to thank my research advisor and mentor, Dr. James Patrone, for his continuous guidance, support, and mentorship throughout the entirety of this project. I would also like to thank Dr. Laurel Habgood for allowing the use of her glovebox as well as her support and mentorship both in and out of the lab. I would also like to thank the members of my committee, Dr. Christopher Fuse and Dr. Brian Mosby, for their time, contributions, and support. I also extend thanks to the Department of Chemistry at Rollins College for supporting this project and for supporting me throughout my undergraduate career. Finally, most importantly, I would like to acknowledge and thank Brownie and Gyle for being perfect, providing Golden Tuesdays, and being my biggest fans.

References

(1) Ogston, A. Micrococcus Poisoning. *J. Anat. Physiol.* **1882**, *17* (Pt 1), 24–58.

(2) Lowy, F. D. Staphylococcus Aureus Infections. *N. Engl. J. Med.* **1998**, *339* (8), 520–532.

(3) Tong, S. Y. C.; Davis, J. S.; Eichenberger, E.; Holland, T. L.; Fowler, V. G. Staphylococcus Aureus Infections: Epidemiology, Pathophysiology, Clinical Manifestations, and Management. *Clin. Microbiol. Rev.* **2015**, *28* (3), 603–661. https://doi.org/10.1128/CMR.00134-14.

(4) Kluytmans, J.; Van Belkum, A.; Verbrugh, H. Nasal Carriage of Staphylococcus Aureus: Epidemiology, Underlying Mechanisms, and Associated Risks. *Clin. Microbiol. Rev.* **1997**, *10* (3), 505–520.

(5) Coates, R.; Moran, J.; Horsburgh, M. J. Staphylococci: Colonizers and Pathogens of Human Skin. *Future Microbiology*. Future Medicine Ltd. January 1, 2014, pp 75–91. https://doi.org/10.2217/fmb.13.145.

(6) Lina, G.; Boutite, F.; Tristan, A.; Bes, M.; Etienne, J.; Vandenesch, F. Bacterial Competition for Human Nasal Cavity Colonization: Role of Staphylococcal Agr Alleles. *Appl. Environ. Microbiol.* **2003**, *69* (1), 18–23. https://doi.org/10.1128/AEM.69.1.18-23.2003.

(7) Foster, T. J.; Geoghegan, J. A.; Ganesh, V. K.; Höök, M. Adhesion, Invasion and Evasion: The Many Functions of the Surface Proteins of Staphylococcus Aureus. *Nat. Rev. Microbiol.* **2014**, *12* (1), 49–62. https://doi.org/10.1038/nrmicro3161.

(8) Boswihi, S. S.; Udo, E. E. Methicillin-Resistant Staphylococcus Aureus : An Update on the Epidemiology, Treatment Options and Infection Control. *Curr. Med. Res. Pract.* **2018**, *8* (1), 18–24. https://doi.org/10.1016/j.cmrp.2018.01.001.

(9) Foster, T. J. The Staphylococcus Aureus "superbug". *J Clin Invest* **2004**, *114* (12), 1693–1696. https://doi.org/10.1172/JCI200422123.7.

(10) Leonard, A. C.; Petrie, L. E.; Cox, G. Bacterial Anti-Adhesives: Inhibition of Staphylococcus Aureus Nasal Colonization. *ACS Infect. Dis.* **2019**, *5* (10), 1668–1681. https://doi.org/10.1021/acsinfecdis.9b00193.

(11) Redi, D.; Raffaelli, C. S.; Rossetti, B.; De Luca, A.; Montagnani, F. Staphylococcus Aureus Vaccine Preclinical and Clinical Development: Current State of the Art. *New Microbiol.* **2018**, *41* (3), 208–213.

(12) Krachler, A. M.; Orth, K. Targeting the Bacteria-Host Interface. *Virulence* **2013**, *4* (4), 284–294. https://doi.org/10.4161/viru.24606.

(13) Cusumano, C. K.; Pinkner, J. S.; Han, Z.; Greene, S. E.; Ford, B. A.; Crowley, J. R.; Henderson, J. P.; Janetka, J. W.; Hultgren, S. J. Treatment and Prevention of Urinary Tract

Infection with Orally Active FimH Inhibitors. *Sci. Transl. Med.* **2011**, *3* (109). https://doi.org/10.1126/scitranslmed.3003021.

(14) Kalas, V.; Hibbing, M. E.; Maddirala, A. R.; Chugani, R.; Pinkner, J. S.; Mydock-McGrane, L. K.; Conover, M. S.; Janetka, J. W.; Hultgren, S. J. Structure-Based Discovery of Glycomimetic FmlH Ligands as Inhibitors of Bacterial Adhesion during Urinary Tract Infection. *Proc. Natl. Acad. Sci. U. S. A.* **2018**, *115* (12), E2819–E2828. https://doi.org/10.1073/pnas.1720140115.

(15) Maddirala, A. R.; Klein, R.; Pinkner, J. S.; Kalas, V.; Hultgren, S. J.; Janetka, J. W. Biphenyl Gal and GalNAc FmlH Lectin Antagonists of Uropathogenic E. Coli (UPEC): Optimization through Iterative Rational Drug Design. *J. Med. Chem.* **2019**, *62* (2), 467–479. https://doi.org/10.1021/acs.jmedchem.8b01561.

(16) Åberg, V.; Almqvist, F. Pilicides - Small Molecules Targeting Bacterial Virulence. *Org. Biomol. Chem.* **2007**, *5* (12), 1827–1834. https://doi.org/10.1039/b702397a.

(17) Svensson, A.; Larsson, A.; Emtenäs, H.; Hedenström, M.; Fex, T.; Hultgren, S. J.; Pinkner, J. S.; Almqvist, F.; Kihlberg, J. Design and Evaluation of Pilicides: Potential Novel Antibacterial Agents Directed against Uropathogenic Escherichia Coli. *ChemBioChem* **2001**, *2* (12), 915–918. https://doi.org/10.1002/1439-7633(20011203)2:12<915::AID-CBIC915>3.0.CO;2-M.

(18) Svensson, M.; Platt, F. M.; Svanborg, C. Glycolipid Receptor Depletion as an Approach to Specific Antimicrobial Therapy. *FEMS Microbiology Letters*. Narnia May 1, 2006, pp 1–8. https://doi.org/10.1111/j.1574-6968.2006.00175.x.

(19) Lacey, K. A.; Geoghegan, J. A.; McLoughlin, R. M. The Role of Staphylococcus Aureus Virulence Factors in Skin Infection and Their Potential as Vaccine Antigens. *Pathogens* **2016**, *5* (22), 1–17. https://doi.org/10.3390/pathogens5010022.

(20) Moscoso, M.; García, P.; Cabral, M. P.; Rumbo, C.; Bou, G. A D-Alanine Auxotrophic Live Vaccine Is Effective against Lethal Infection Caused by Staphylococcus Aureus. *Virulence* **2018**, *9* (1), 604–620. https://doi.org/10.1080/21505594.2017.1417723.

(21) Singh, R. K.; Tiwari, S. P.; Rai, A. K.; Mohapatra, T. M. Cyanobacteria: An Emerging Source for Drug Discovery. *J. Antibiot. (Tokyo).* **2011**, *64* (6), 401–412. https://doi.org/10.1038/ja.2011.21.

(22) Olaizola, M. Commercial Development of Microalgal Biotechnology: From the Test Tube to the Marketplace. *Biomol. Eng.* **2003**, No. 20, 459–466. https://doi.org/10.1016/S1389-0344(03)00076-5.

(23) Schopf, J. W. Fossil Evidence of Archaean Life. *Philos. Trans. R. Soc. B Biol. Sci.* **2006**, *361* (1470), 869–885. https://doi.org/10.1098/rstb.2006.1834.

(24) Chlipala, G. E.; Mo, S.; Orjala, J. Chemodiversity in Freshwater and Terrestrial Cyanobacteria—A Source for Drug Discovery. *Curr. Drug Targets* **2011**, *12* (11), 1654–1673.

(25) González-Medina, M.; Medina-Franco, J. L. Chemical Diversity of Cyanobacterial Compounds: A Chemoinformatics Analysis. *ACS Omega* **2019**, *4* (4), 6229–6237. https://doi.org/10.1021/acsomega.9b00532.

(26) Nozzi, N. E.; Oliver, J. W. K.; Atsumi, S. Cyanobacteria as a Platform for Biofuel Production. *Front. Bioeng. Biotechnol.* **2013**, *1*, 1–6. https://doi.org/10.3389/fbioe.2013.00007.

(27) Li, Z.; Guo, M. Healthy Efficacy of Nostoc Commune Vaucher. *Oncotarget* **2018**, *9* (18), 14669–14679. https://doi.org/10.18632/oncotarget.23620.

(28) Nunnery, J. K.; Mevers, E.; Gerwick, W. H. Biologically Active Secondary Metabolites from Marine Cyanobacteria. *Curr. Opin. Biotechnol.* **2010**, *21*, 787–793. https://doi.org/10.1016/j.copbio.2010.09.019.
(29) Bui, H. T. N.; Jansen, R.; Pham, H. T. L.; Mundt, S. Carbamidocyclophanes A-E, Chlorinated Paracyclophanes with Cytotoxic and Antibiotic Activity from the Vietnamese Cyanobacterium Nostoc Sp. *J. Nat. Prod.* **2007**, *70* (4), 499–503. https://doi.org/10.1021/np060324m.
(30) El-Sheekh, M. M.; Osman, M. E. H.; Dyab, M. A.; Amer, M. S. Production and Characterization of Antimicrobial Active Substance from the Cyanobacterium Nostoc Muscorum. *Environ. Toxicol. Pharmacol.* **2006**, *21* (1), 42–50. https://doi.org/10.1016/j.etap.2005.06.006.
(31) Asthana, R. K.; Srivastava, A.; Singh, A. P.; Deepali; Singh, S. P.; Nath, G.; Srivastava, R.; Srivastava, B. S. Identification of an Antimicrobial Entity from the Cyanobacterium Fischerella Sp. Isolated from Bark of Azadirachta Indica (Neem) Tree. *J. Appl. Phycol.* **2006**, *18* (1), 33–39. https://doi.org/10.1007/s10811-005-9011-9.
(32) Brumley, D.; Spencer, K. A.; Gunasekera, S. P.; Sauvage, T.; Biggs, J.; Paul, V. J.; Luesch, H. Isolation and Characterization of Anaephenes A-C, Alkylphenols from a Filamentous Cyanobacterium (Hormoscilla Sp., Oscillatoriales). *J. Nat. Prod.* **2018**, *81* (12), 2716–2721. https://doi.org/10.1021/acs.jnatprod.8b00650.
(33) Luesch, H.; Pangilinan, R.; Yoshida, W. Y.; Moore, R. E.; Paul, V. J. Pitipeptolides A and B, New Cyclodepsipeptides from the Marine Cyanobacterium Lyngbya Majuscula. *J. Nat. Prod.* **2001**, *64* (3), 304–307. https://doi.org/10.1021/np000456u.
(34) Edwards, D. J.; Marquez, B. L.; Nogle, L. M.; McPhail, K.; Goeger, D. E.; Roberts, M. A.; Gerwick, W. H. Structure and Biosynthesis of the Jamaicamides, New Mixed Polyketide-Peptide Neurotoxins from the Marine Cyanobacterium Lyngbya Majuscula. *Chem. Biol.* **2004**, *11* (6), 817–833.
(35) Kwan, J. C.; Meickle, T.; Ladwa, D.; Teplitski, M.; Paul, V.; Luesch, H. Lyngbyoic Acid, a "Tagged" Fatty Acid from a Marine Cyanobacterium, Disrupts Quorum Sensing in Pseudomonas Aeruginosa. *Mol Biosyst.* **2011**, *7* (4), 1205–1216. https://doi.org/10.1039/b000000x/The.
(36) Cardellina, J. H.; Marner, F. J.; Moore, R. E. Malyngamide A, A Novel Chlorinated Metabolite of the Marine Cyanophyte Lyngbya Majuscula. *J. Am. Chem. Soc.* **1979**, *101* (1), 240–242. https://doi.org/10.1021/ja00495a051.
(37) Papendorf, O.; König, G. M.; Wright, A. D. Hierridin B and 2,4-Dimethoxy-6-Heptadecyl-Phenol, Secondary Metabolites from the Cyanobacterium Phormidium Ectocarpi with Antiplasmodial Activity. *Phytochemistry* **1998**, *49* (8), 2383–2386. https://doi.org/10.1016/S0031-9422(98)00440-3.
(38) Leão, P. N.; Costa, M.; Ramos, V.; Pereira, A. R.; Fernandes, V. C.; Domingues, V. F.; Gerwick, W. H.; Vasconcelos, V. M.; Martins, R. Antitumor Activity of Hierridin B, a Cyanobacterial Secondary Metabolite Found in Both Filamentous and Unicellular Marine Strains. *PLoS One* **2013**, *8* (7), 1–8. https://doi.org/10.1371/journal.pone.0069562.
(39) Johansson Seechurn, C. C. C.; Kitching, M. O.; Colacot, T. J.; Snieckus, V. Palladium-Catalyzed Cross-Coupling: A Historical Contextual Perspective to the 2010 Nobel Prize. *Angew. Chemie - Int. Ed.* **2012**, *51* (21), 5062–5085. https://doi.org/10.1002/anie.201107017.
(40) Miyaura, N.; Yamada, K.; Suzuki, A. A New Stereospecific Cross-Coupling by the

Palladium-Catalyzed Reaction of 1-Alkenylboranes with 1-Alkenyl or 1- Alkynyl Halides. *Tetrahedron Lett.* **1979**, *20* (36), 3437–3440.
(41) Kurti, L.; Czako, B. Suzuki Cross-Coupling. In *Strategic Applications of Named Reactions in Organic Synthesis*; Elsevier Science, 2005; pp 448–449.
(42) Crimmins, M. T.; Haley, M. W.; O'Bryan, E. A. Formal Synthesis of (+)-Sorangicin A. *Org. Lett.* **2011**, *13* (17), 4712–4715. https://doi.org/10.1021/ol201920j.
(43) Paul, D.; Saha, S.; Goswami, R. K. Total Synthesis of Pestalotioprolide e and Structural Revision of Pestalotioprolide F. *Org. Lett.* **2018**, *20* (15), 4606–4609. https://doi.org/10.1021/acs.orglett.8b01894.
(44) Kock, M.; Lindel, T. Diastereoselective Total Synthesis of Raputindole A. *Org. Lett.* **2018**, *20* (17), 5444–5447. https://doi.org/10.1021/acs.orglett.8b02349.
(45) Evans, D. A.; Ng, H. P.; Rieger, D. L. Total Synthesis of the Macrolide Antibiotic Rutamycin B. *J. Am. Chem. Soc.* **1993**, *115* (24), 11446–11459. https://doi.org/10.1021/ja00077a049.
(46) Sancéau, J. Y.; Maltais, R.; Poirier, D.; Marette, A. Total Synthesis of the Antidiabetic (Type 2) Lipid Mediator Protectin DX/PDX. *J. Org. Chem.* **2019**, *84* (2), 495–505. https://doi.org/10.1021/acs.joc.8b01973.
(47) Coombs, J. R.; Zhang, L.; Morken, J. P. Enantiomerically Enriched Tris(Boronates): Readily Accessible Conjunctive Reagents for Asymmetric Synthesis. *J. Am. Chem. Soc.* **2014**, *136* (46), 16140–16143. https://doi.org/10.1021/ja510081r.
(48) Zhan, Y.; Liu, T.; Ren, J.; Wang, Z. Lewis Acid-Catalyzed Intramolecular [3+2] Cross-Cycloaddition of Aziridine 2,2-Diesters with Conjugated Dienes for Construction of Aza-[n.2.1] Skeletons. *Chem. - A Eur. J.* **2017**, *23* (71), 17862–17866. https://doi.org/10.1002/chem.201704695.
(49) Hodgson, D. M.; Labande, A. H.; Pierard, F. Y. T. M.; Expósito Castro, M. A. The Scope of Catalytic Enantioselective Tandem Carbonyl Ylide Formation - Intramolecular [3 + 2] Cycloadditions. *J. Org. Chem.* **2003**, *68* (16), 6153–6159. https://doi.org/10.1021/jo0343735.
(50) Goh, S. S.; Baars, H.; Gockel, B.; Anderson, E. A. Metal-Catalyzed Syntheses of Abridged CDE Rings of Rubriflordilactones A and B. *Org. Lett.* **2012**, *14* (24), 6278–6281. https://doi.org/10.1021/ol303041j.
(51) Wang, Y. F.; Gao, Y. R.; Mao, S.; Zhang, Y. L.; Guo, D. D.; Yan, Z. L.; Guo, S. H.; Wang, Y. Q. Wacker-Type Oxidation and Dehydrogenation of Terminal Olefins Using Molecular Oxygen as the Sole Oxidant without Adding Ligand. *Org. Lett.* **2014**, *16* (6), 1610–1613. https://doi.org/10.1021/ol500218p.
(52) Ang, N. W. J.; Buettner, C. S.; Docherty, S.; Bismuto, A.; Carney, J. R.; Docherty, J. H.; Cowley, M. J.; Thomas, S. P. Borane-Catalysed Hydroboration of Alkynes and Alkenes. *Synthesis (Stuttg).* **2018**, *50*, 803–808.
(53) Layton, M. E.; Morales, C. A.; Shair, M. D. Biomimetic Synthesis of (−)-Longithorone A. *J. Am. Chem. Soc.* **2002**, *124* (5), 773–775. https://doi.org/10.1021/ja016585u.